

Finite element analysis of elastic properties of metamaterials based on triply periodic minimal surfaces

A.I. Borovkov ¹,  L.B. Maslov ^{1,2},  M.A. Zhmaylo ¹ ,  F.D. Tarasenko ¹, 
L.S. Nezhinskaya ¹, 

¹ Peter the Great St. Petersburg Polytechnic University, St. Petersburg, Russia

² Ivanovo State Power Engineering University n.a. V.I. Lenin, Ivanovo, Russia

✉ zhmaylo@compmechlab.com

ABSTRACT

The paper considers models of porous structures based on triply periodic minimal surfaces, which are an example of additively produced metamaterials of a new topological class. A numerical technology for the construction of metamaterial periodicity cell based on surface structures is developed, which ensures the periodic boundary conditions fulfilment on finite element meshes. The elastic properties of metamaterials have been calculated by the method of direct numerical homogenization at the periodicity cell meso-level. The dependences of the effective properties on the volume fraction of the metamaterial solid phase are revealed and it is noted that their proper description requires an orthotropic material model. It is shown that the considered types of metamaterials demonstrate strongly nonlinear dependence of elastic properties on the relative density or volume fraction of the solid phase of the metamaterial. The curvature of the curve is more pronounced for values of relative density less than 50 %, which may indicate a pronounced influence of the topological characteristics of the cell on the behaviour of the metamaterial at the meso-level. When analysing the Poisson's ratios, a significant variation in their behaviour for different types of metamaterials is observed. The reason for this phenomenon may be the more pronounced influence of the unit cell topology on the transverse deformations. The consequence of this phenomenon is the apparent existence of stationary points corresponding to the maximum or minimum achievable values of the Poisson's ratio, which can be useful in problems where its value has a significant influence on the global result.

KEYWORDS

metamaterials • porous structures • finite element analysis • homogenization • periodic cell • elastic moduli

Acknowledgements. This work has been supported by the Russian Science Foundation grant No. 23-19-00882, <https://rscf.ru/project/23-19-00882/>.

Citation: Borovkov AI, Maslov LB, Zhmaylo MA, Tarasenko FD, Nezhinskaya LS. Finite element analysis of elastic properties of metamaterials based on triply periodic minimal surfaces. *Materials Physics and Mechanics*. 2024;52(2): 11–29.

http://dx.doi.org/10.18149/MPM.5222024_2

Introduction

The concept of “metamaterials” has emerged relatively recently to denote a new promising class of artificial porous structures that can be produced using additive manufacturing technologies. It can be said that the precursors of modern metamaterials produced on 3D printers using selective laser melting technologies [1] were foamy highly porous polymeric materials of low and ultralow density with random distribution of voids and material in the volume, known since the end of the previous century [2,3].

The characteristic features of modern metamaterials are the possibility of designing structures with specific mechanical [4,5], acoustic [6], electromagnetic [7], poroelastic [8],

biophysical [9,10] and other material properties, which are determined by the type and parameters of the internal structure of a typical repeating unit cell forming the metamaterial. Moreover, by changing the characteristics of the cell, it becomes possible to control the effective physical and mechanical properties of the structure in any spatial direction to create so-called gradient metamaterials [11].

An actual direction of research in the field of mechanics of metamaterials is the study of dependence of macroscopic physical and mechanical properties of a periodic structure of a metamaterial on topological parameters of this structure at the meso-level of the periodicity cell. The main purpose of such studies is to investigate and develop methods of metamaterial design for given operating conditions, as a rule, by varying topological parameters and their distribution in accordance with the obtained dependences. For example, in [12,13], models and samples with a unique combination of parameters and shape of the periodic structure are presented, providing effective mechanical properties close to bone tissue.

If we exclude from consideration porous materials with irregular distribution of pore channels, the existing models of metamaterials as periodic structures can be divided into two main groups differing by the type of characteristic basic elements forming the periodicity cell of the metamaterial. The first group includes metamaterials whose representative volume element, or periodicity cell, is formed from beams or rod elements [14]. Such structures were inspired by the crystal structures of metals and, often, repeat some form of spatial symmetry: volume-centred lattice (VCC), face-centred cubic lattice (FCC), hexagonal closely packed (HCP) and others. The second group includes metamaterials whose periodicity cell is a shell structure and is based on complex curved surfaces of a given thickness [15].

For “beam” metamaterials, the issue of the influence of topological properties on quasi-static mechanical properties is represented by a broad front of studies, where typical periodicity cells are considered and the influence of the filling density on the effective properties is studied. The works use both analytical models, such as Euler-Bernoulli [16] or Timoshenko [17] rod models, which allow predicting macroscopic elastic properties without virtual tests, and direct numerical homogenisation based on the finite element method (FEM) implemented in commercial software tools [18–20], to calculate the elastic properties of metamaterials.

Prototypes of metamaterials based on surface elements have appeared relatively recently and immediately gained popularity among researchers due to their advantages over metamaterials based on rod elements in a number of specific applications, where a developed internal structure formed by a branched system of interconnected pore channels is required without abrupt changes in their curvature. Metamaterials based on triply periodic minimal surfaces (TPMS) have taken a special place among them [21]. TPMS represent a set of periodically repeating implicit surfaces with zero mean curvature, which means local minimisation of the surface area for a three-dimensional region with some given boundary. The metamaterial based on TPMS's consists of infinite, non-overlapping shells of a given thickness, repeating in the directions of three coordinate axes with a given frequency.

Due to the large specific area of internal surfaces, TPMS-metamaterials can be used as energy absorbers (kinetic, thermal, acoustic wave energy, microwave electromagnetic

waves), chemical microreactors, membrane devices, and heat-generating elements [21]. Currently, the use of such metamaterials in the field of biomedical applications as bone scaffold or implant is being actively studied. This is due to the fact that for effective osteointegration, artificial bone tissue substitutes should possess a branched system of open-type pore channels for migration and transformation of active cells into bone substance [22], but, at the same time, have sufficient strength to ensure the functionality of organs, especially the human musculoskeletal apparatus [23]. The use of metamaterials of this type has potential advantages over the “bar” type due to the larger area of internal surfaces with a curvature close to the curvature of the trabecular bone tissue structure having a branched system of pore channels [24,25], which is necessary to ensure effective regeneration of biological tissue in the inner space of the scaffold [26].

Among the basic parameters of metamaterials related to various physical applications, studies of mechanical characteristics have received the most attention in the publications. Whether TPMS-based porous structures are used as bone scaffolds, energy absorbers or heat exchangers, the determination of basic mechanical characterisation is required to ensure the reliability of the structures. Young’s and shear moduli, Poisson’s ratios, especially in the case of anisotropy of elastic properties, are the main mechanical parameters that are the subject of studies [27].

Porous structures can be considered as a special kind of composite material with solid material phase and air phase [28]. Consequently, the Hashin-Strikman upper boundary can be effectively applied to evaluate the mechanical properties of TPMS’s. It is shown that, compared to lattice structures, the value of the bulk modulus of elasticity of metamaterials based on TPMS is much closer to the theoretical limit [29].

The effective, or relative, density, which is related to the porosity or volume content of the material, acts as the main integral characteristic that determines the geometrical features of the metamaterial. In this regard, there are a number of studies devoted to the evaluation of this influence. The essence of the studies is to determine the relationship between the effective characteristics (elastic moduli and ultimate stresses) and the relative density also on the basis of scaling laws [30]. According to numerical calculations using FEM and full-scale compression tests, there is a monotonic smooth dependence of the effective elastic moduli on the relative density of the metamaterial [31,32].

It is worth noting that different metamaterials in general and TPMS-based metamaterials in particular can have the same relative density, but show different effective properties. This effect is due to the fact that relative density is not an exhaustive characteristic, and the properties depend on other topological parameters as well. The influence of topological parameters describing triply periodic minimal surfaces on elastic moduli and degree of anisotropy was investigated in [33]. According to the study, it was shown that the elastic modulus and anisotropic properties can be controlled simultaneously by varying different unit cell parameters.

In addition to the analysis of effective elastic properties, significant research attention is paid to the issues of static strength and loss of stability of metamaterials, which is essential for lattice structures formed by beam elements operating in compression [34]. Methods for non-topological optimization of metamaterials to ensure a given strength at minimum weight of the lattice structure are also being developed [35], in particular for biomedical applications of metamaterials [36].

The numerical algorithms for parametric optimization of the lattice structure proposed in [35] were developed in [37] for a special type of metamaterial based on a basic cell containing a pore of varying elliptical shape and orientation. The proposed technique demonstrated its success on the example of the stem of a hip joint endoprosthesis, allowing to reduce the volume of material by 9-11 % depending on the type of implant while maintaining the strength of the structure.

Despite the fact that the studies demonstrate the high potential of the described structures [38], the degree of study of such metamaterials in the context of the previously described issues is much lower in comparison with the "beam" type of cells for a number of reasons: non-triviality of creating parameterised geometrical models, complexity of additive manufacturing, limited number of basic geometrical parameters to be varied.

The paper will consider computer models of metamaterials having periodicity cells with internal structure formed by shells based on thrice periodic minimal surfaces. Using the method of direct finite-element homogenisation, the effective elastic properties of the developed metamaterial models will be calculated depending on the characteristic parameters of their internal structure.

Materials and methods

Theoretical aspects of homogenization technique

Homogenisation is a method of estimating equivalent macroscopic properties, where a relatively homogeneous material is obtained from a heterogeneous material, and the properties of the homogeneous material are globally the same as those of the heterogeneous material. Such properties of the metamaterial are called effective properties. The results obtained for one cell can be generalised for the whole material due to its periodic structure.

The stress and strain values averaged over the elementary representative element are defined by the formulas:

$$\langle \sigma_{ij} \rangle = \frac{1}{V} \int_V \sigma_{ij} dV, \quad \langle \varepsilon_{ii} \rangle = \frac{1}{V} \int_V \varepsilon_{ii} dV, \quad \langle \gamma_{ij} \rangle = \frac{1}{V} \int_V \gamma_{ij} dV, \quad (1)$$

where V are the volume of the representative volume element (RVE).

The stresses and strains averaged over a representative volume element in points of a porous material, which is considered as a homogeneous continuous medium, as a result of homogenisation are related by the equations of the generalised Hooke's law written in the principal axes of material symmetry X, Y, Z of the stress and strain tensors:

$$\begin{aligned} E_x \langle \varepsilon_{xx} \rangle &= \langle \sigma_{xx} \rangle - \nu_{xy} \langle \sigma_{yy} \rangle - \nu_{xz} \langle \sigma_{zz} \rangle, \\ E_y \langle \varepsilon_{yy} \rangle &= -\nu_{yx} \langle \sigma_{xx} \rangle + \langle \sigma_{yy} \rangle - \nu_{yz} \langle \sigma_{zz} \rangle, \\ E_z \langle \varepsilon_{zz} \rangle &= -\nu_{zx} \langle \sigma_{xx} \rangle - \nu_{zy} \langle \sigma_{yy} \rangle + \langle \sigma_{zz} \rangle, \\ G_{xy} \langle \gamma_{xy} \rangle &= \langle \sigma_{xy} \rangle, \\ G_{yz} \langle \gamma_{yz} \rangle &= \langle \sigma_{yz} \rangle, \\ G_{xz} \langle \gamma_{xz} \rangle &= \langle \sigma_{xz} \rangle, \end{aligned} \quad (2)$$

here E_x, E_y, E_z are effective Young's moduli of the elementary cell; $\nu_{xy}, \nu_{yx}, \nu_{yz}, \nu_{zy}, \nu_{xz}$ and ν_{zx} are effective Poisson's ratios; G_{xy}, G_{yz} and G_{xz} are effective shear moduli.

Compliance matrix $[C]$, which defines the relation between stresses and strains, can be written in the following way according to Eq. (2):

$$[C] = \begin{pmatrix} \frac{1}{E_x} & -\frac{\nu_{yx}}{E_y} & -\frac{\nu_{zx}}{E_z} & 0 & 0 & 0 \\ -\frac{\nu_{xy}}{E_x} & \frac{1}{E_y} & -\frac{\nu_{zy}}{E_z} & 0 & 0 & 0 \\ -\frac{\nu_{xz}}{E_x} & -\frac{\nu_{yz}}{E_y} & \frac{1}{E_z} & 0 & 0 & 0 \\ 0 & 0 & 0 & \frac{1}{G_{xy}} & 0 & 0 \\ 0 & 0 & 0 & 0 & \frac{1}{G_{yz}} & 0 \\ 0 & 0 & 0 & 0 & 0 & \frac{1}{G_{xz}} \end{pmatrix}. \quad (3)$$

Apart from the Eq. (2), Hooke's law can be written in the form more familiar to continuum mechanics as an expression of stress through strain:

$$\begin{pmatrix} \langle \sigma_{xx} \rangle \\ \langle \sigma_{yy} \rangle \\ \langle \sigma_{zz} \rangle \\ \langle \sigma_{xy} \rangle \\ \langle \sigma_{yz} \rangle \\ \langle \sigma_{xz} \rangle \end{pmatrix} = \begin{pmatrix} D_{11} & D_{12} & D_{13} & 0 & 0 & 0 \\ D_{21} & D_{22} & D_{23} & 0 & 0 & 0 \\ D_{31} & D_{32} & D_{33} & 0 & 0 & 0 \\ 0 & 0 & 0 & D_{44} & 0 & 0 \\ 0 & 0 & 0 & 0 & D_{55} & 0 \\ 0 & 0 & 0 & 0 & 0 & D_{66} \end{pmatrix} \begin{pmatrix} \langle \varepsilon_{xx} \rangle \\ \langle \varepsilon_{yy} \rangle \\ \langle \varepsilon_{zz} \rangle \\ \langle \gamma_{xy} \rangle \\ \langle \gamma_{yz} \rangle \\ \langle \gamma_{xz} \rangle \end{pmatrix}, \quad (4)$$

where $[D]$ is a stiffness matrix corresponding to 4th rank the elastic moduli tensor, which is inverse to the compliance matrix:

$$[D] = \begin{pmatrix} D_{11} & D_{12} & D_{13} & 0 & 0 & 0 \\ D_{21} & D_{22} & D_{23} & 0 & 0 & 0 \\ D_{31} & D_{32} & D_{33} & 0 & 0 & 0 \\ 0 & 0 & 0 & D_{44} & 0 & 0 \\ 0 & 0 & 0 & 0 & D_{55} & 0 \\ 0 & 0 & 0 & 0 & 0 & D_{66} \end{pmatrix}, [D] = [C]^{-1}. \quad (5)$$

Six numerical tests are required to determine the independent constants: three in uniaxial tension and three in shear. The average stresses for numerical homogenisation can be found as the ratio of the reaction force F_k applied to the face of the unit cell to its area S :

$$\langle \sigma_{ij}^k \rangle = \frac{F_k}{S} \quad (6)$$

where $i, j \in \{x, y, z\}$, $k \in \{x, y, z, xy, yz, xz\}$.

The index k in Eq. (6) corresponds to the experiment performed: X-stretching along the X -axis, Y-stretching along the Y -axis, Z-stretching along the Z -axis, XY-shear in the XY -plane, YZ-shear in the YZ -plane, XZ-shear in the XZ -plane. When considering each experiment separately, the Eq. (6) will take a simplified form, where $\langle \sigma_{ij}^x \rangle$, $\langle \sigma_{ij}^y \rangle$, $\langle \sigma_{ij}^z \rangle$ are averaged stress values for the cases of uniaxial tension along X , Y , and Z axes correspondingly, $\langle \sigma_{ij}^{xy} \rangle$, $\langle \sigma_{ij}^{yz} \rangle$, $\langle \sigma_{ij}^{xz} \rangle$ are averaged stress values for the cases of shear in XY , YZ and ZX planes correspondingly (here $i, j \in \{x, y, z\}$). As a result of application of Eqs. (4) and (6), the following expressions can be formulated:

$$A \begin{pmatrix} D_{11} \\ D_{21} \\ D_{31} \\ 0 \\ 0 \\ 0 \end{pmatrix} = \begin{pmatrix} \langle \sigma_{xx}^x \rangle \\ \langle \sigma_{yy}^x \rangle \\ \langle \sigma_{zz}^x \rangle \\ 0 \\ 0 \\ 0 \end{pmatrix}, \quad A \begin{pmatrix} D_{12} \\ D_{22} \\ D_{32} \\ 0 \\ 0 \\ 0 \end{pmatrix} = \begin{pmatrix} \langle \sigma_{xx}^y \rangle \\ \langle \sigma_{yy}^y \rangle \\ \langle \sigma_{zz}^y \rangle \\ 0 \\ 0 \\ 0 \end{pmatrix}, \quad A \begin{pmatrix} D_{13} \\ D_{23} \\ D_{33} \\ 0 \\ 0 \\ 0 \end{pmatrix} = \begin{pmatrix} \langle \sigma_{xx}^z \rangle \\ \langle \sigma_{yy}^z \rangle \\ \langle \sigma_{zz}^z \rangle \\ 0 \\ 0 \\ 0 \end{pmatrix}, \quad (7a)$$

$$A \begin{pmatrix} 0 \\ 0 \\ 0 \\ D_{44} \\ 0 \\ 0 \end{pmatrix} = \begin{pmatrix} 0 \\ 0 \\ \langle \sigma_{xy}^{xy} \rangle \\ 0 \\ 0 \\ 0 \end{pmatrix}, \quad A \begin{pmatrix} 0 \\ 0 \\ 0 \\ 0 \\ D_{55} \\ 0 \end{pmatrix} = \begin{pmatrix} 0 \\ 0 \\ 0 \\ \langle \sigma_{yz}^{yz} \rangle \\ 0 \\ 0 \end{pmatrix}, \quad A \begin{pmatrix} 0 \\ 0 \\ 0 \\ 0 \\ 0 \\ D_{66} \end{pmatrix} = \begin{pmatrix} 0 \\ 0 \\ 0 \\ 0 \\ 0 \\ \langle \sigma_{xz}^{xz} \rangle \end{pmatrix}, \quad (7b)$$

where A is a value of longitudinal strain along one of the main orthotropy axes or value of transverse shear strain in one of the main orthotropy planes; hereinafter we will take the value of $A = 0.001$.

Based on the results of six experiments, according to relations (7a) and (7b), we obtain the unknown components of the stiffness matrix D_{ij} . Then we determine the compliance matrix by Eq. (5), after which all unknown elastic constants can be determined using Eq. (3):

$$\begin{aligned} E_x &= \frac{1}{C_{11}}, E_y = \frac{1}{C_{22}}, E_z = \frac{1}{C_{33}}, \\ G_{xy} &= \frac{1}{C_{44}}, G_{yz} = \frac{1}{C_{55}}, G_{xz} = \frac{1}{C_{66}}, \\ \nu_{xy} &= -\frac{C_{21}}{C_{11}}, \nu_{xz} = -\frac{C_{31}}{C_{11}}, \nu_{yz} = -\frac{C_{32}}{C_{22}}. \end{aligned} \quad (8)$$

Due to the fact that the metamaterial is a periodic structure, numerical experiments should be carried out with boundary conditions different from the traditional ones. Periodic boundary conditions sufficiently describe the three-dimensional symmetry of the structure, and also provide a more adequate description of deformations, since they reflect the direct influence of deformation of the cell under consideration on its neighbours.

The periodic boundary conditions represent the same displacements of each pair of nodes on opposite faces of a periodic cell of size $L_x \times L_y \times L_z$. Three tensile tests and three shear tests are considered sequentially to determine the material parameters under the boundary conditions described above.

For the numerical uniaxial tensile tests along the X , Y and Z axes, the following periodicity boundary conditions must be satisfied on pairs of opposite sides of the representative element, respectively.

Tension along the X -axis:

$$\mathbf{u}|_{x=0} - \mathbf{u}|_{x=L_x} = A\mathbf{i}, \quad \mathbf{u}|_{y=0} - \mathbf{u}|_{y=L_y} = 0, \quad \mathbf{u}|_{z=0} - \mathbf{u}|_{z=L_z} = 0. \quad (9a)$$

Tension along the Y -axis:

$$\mathbf{u}|_{x=0} - \mathbf{u}|_{x=L_x} = 0, \quad \mathbf{u}|_{y=0} - \mathbf{u}|_{y=L_y} = A\mathbf{j}, \quad \mathbf{u}|_{z=0} - \mathbf{u}|_{z=L_z} = 0. \quad (9b)$$

Tension along the Z -axis:

$$\mathbf{u}|_{x=0} - \mathbf{u}|_{x=L_x} = 0, \quad \mathbf{u}|_{y=0} - \mathbf{u}|_{y=L_y} = 0, \quad \mathbf{u}|_{z=0} - \mathbf{u}|_{z=L_z} = A\mathbf{k}. \quad (9c)$$

here \mathbf{u} is a displacement vector for the RVE; $\mathbf{i}, \mathbf{j}, \mathbf{k}$ are orfs of the coordinate system corresponding to axes X, Y, Z .

To perform three shear tests in the XY , YZ and XZ planes, the periodic boundary conditions on pairs of opposite sides of the representative element will take the following form.

Shear in the XY -plane:

$$\mathbf{u}|_{x=0} - \mathbf{u}|_{x=L_x} = A\mathbf{j}, \mathbf{u}|_{y=0} - \mathbf{u}|_{y=L_y} = A\mathbf{i}, \mathbf{u}|_{z=0} - \mathbf{u}|_{z=L_z} = 0. \quad (10a)$$

Shear in the YZ -plane:

$$\mathbf{u}|_{x=0} - \mathbf{u}|_{x=L_x} = 0, \mathbf{u}|_{y=0} - \mathbf{u}|_{y=L_y} = Ak, \mathbf{u}|_{z=0} - \mathbf{u}|_{z=L_z} = Aj. \quad (10b)$$

Shear in the ZX -plane:

$$\mathbf{u}|_{x=0} - \mathbf{u}|_{x=L_x} = Ak, \mathbf{u}|_{y=0} - \mathbf{u}|_{y=L_y} = 0, \mathbf{u}|_{z=0} - \mathbf{u}|_{z=L_z} = A\mathbf{i}. \quad (10c)$$

The presented algorithm is implemented in the EasyPBC plug-in [39] for the finite element analysis software package Abaqus CAE, where all the necessary calculations were performed. The work of the plug-in consists in defining sets of nodes on opposite faces of the periodicity cell and sequential application of periodic boundary conditions (9) and (10) to them. Consecutive numerical solutions of three uniaxial tensile problems along each of the coordinate axes and three pure shear problems in each of the coordinate planes are then carried out. Schemes of the problems for tension along the Z coordinate axis and shear in the YZ coordinate plane are shown in Fig. 1.

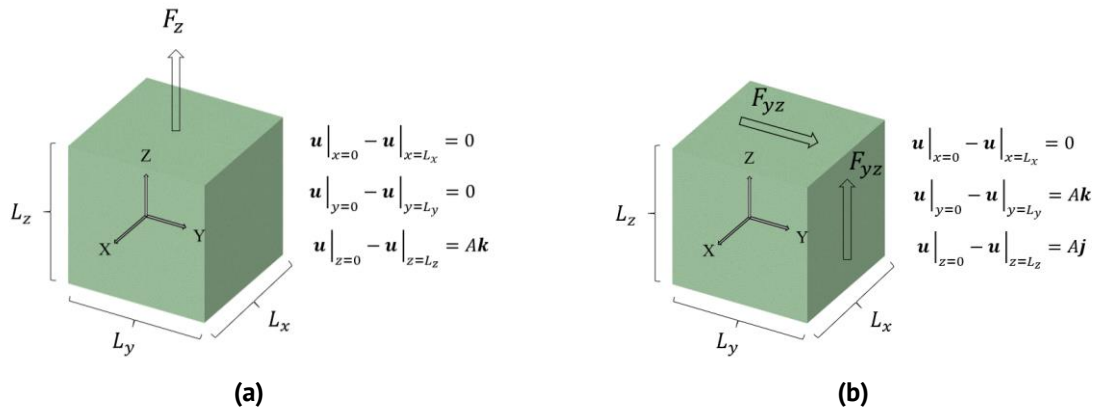


Fig. 1. Problem statements of uniaxial tension along the Z -axis (a) and shear in the YZ -plane (b) to perform homogenization

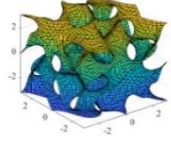
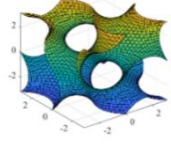
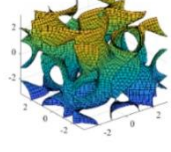
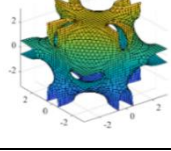
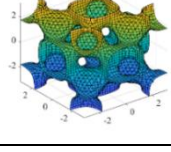
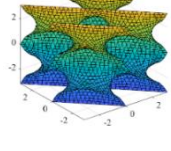
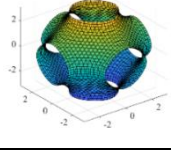
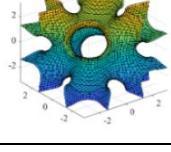
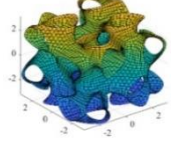
After the calculations at the meso-level of the elementary representative volume, the effective elastic characteristics of the metamaterial according to Eq. (8) are calculated from the obtained stress values (7) and given deformations.

Triply periodic minimal surfaces

In this paper we consider nine well-known types of triply periodic minimal surfaces described by functions $F(x, y, z)$ [40] (Table 1).

Geometrical models of elementary cells of metamaterial based on TPMS are developed under the assumption that the interface surface of solid material and air of inhomogeneous structure is described by an implicit equation of the following form $F(x, y, z) = C$.

Table 1. Parameters of triply periodic minimal surfaces

Name	Surface shape	Mathematical expression $F(x, y, z)$
Fischer Koch		$\sin(\omega_x x) \cos(\omega_y y) \cos(2\omega_z z) + \cos(2\omega_x x) \sin(\omega_y y) \cos(\omega_z z) + \cos(\omega_x x) \cos(2\omega_y y) \sin(\omega_z z)$
Gyroid		$\cos(\omega_x x) \sin(\omega_y y) + \sin(\omega_x x) \cos(\omega_z z) + \cos(\omega_y y) \sin(\omega_z z)$
Lidinoid		$\sin(\omega_x x) \sin(2\omega_y y) \cos(\omega_z z) + \sin(2\omega_x x) \cos(\omega_y y) \sin(\omega_z z) - \cos(2\omega_y y) \cos(2\omega_z z) + \cos(\omega_x x) \sin(\omega_y y) \sin(2\omega_z z) - \cos(2\omega_x x) \cos(2\omega_y y) - \cos(2\omega_x x) \cos(2\omega_z z)$
Neovius		$4\cos(\omega_x x) \cos(\omega_y y) \cos(\omega_z z) + 3(\cos(\omega_x x) + \cos(\omega_y y) + \cos(\omega_z z))$
Primary IWP		$4\cos(\omega_x x) \cos(\omega_y y) \cos(\omega_z z) - (\cos(2\omega_x x) \cos(2\omega_y y) + \cos(2\omega_x x) \cos(2\omega_z z) + \cos(2\omega_y y) \cos(2\omega_z z))$
Schwarz D		$\sin(\omega_x x) \sin(\omega_y y) \sin(\omega_z z) + \sin(\omega_x x) \cos(\omega_y y) \cos(\omega_z z) + \cos(\omega_x x) \sin(\omega_y y) \cos(\omega_z z) + \cos(\omega_x x) \cos(\omega_y y) \sin(\omega_z z)$
Schwarz P		$\cos(\omega_x x) + \cos(\omega_y y) + \cos(\omega_z z)$
Secondary IWP		$2(\cos(\omega_x x) \cos(\omega_y y) + \cos(\omega_x x) \cos(\omega_z z) + \cos(\omega_y y) \cos(\omega_z z)) - (\cos(2\omega_x x) + \cos(2\omega_y y) + \cos(2\omega_z z))$
Split P		$-0,2(\cos(2\omega_x x) \cos(2\omega_y y) + \cos(2\omega_x x) \cos(2\omega_z z) + \cos(2\omega_y y) \cos(2\omega_z z)) + \sin(2\omega_x x) \cos(\omega_y y) \sin(\omega_z z) - 0,4(\cos(2\omega_x x) + \cos(2\omega_y y) + \cos(2\omega_z z)) + \cos(\omega_x x) \sin(\omega_y y) \sin(2\omega_z z) + 1,1(\sin(\omega_x x) \sin(2\omega_y y) \cos(\omega_z z))$

The constant C allows to vary the ratio of solid material to air in the structure and serves as a parameter determining the volume fraction of the unit cell. By assuming the condition $F(x, y, z) > C$ or $F(x, y, z) < C$, we can switch between considering only one part of the porous material, namely the solid phase or air [41]. At $C = 0$ values of the volumes of solid material and air in the unit cell are equal to each other.

The influence of constant C on the surface appearance is explained in Fig. 2 at fixed repetition frequencies along the coordinate axes for two typical Fischer Koch and Schwarz P TPMS's. It can be observed that varying the constant between 0 and 0.5 changes the characteristic dimensions of the surface structures without changing the topology. However, when C approaches 1, the initial topology (at $C = 0$) changes significantly, including the fact that it may become unsuitable for construction of a metamaterial model.

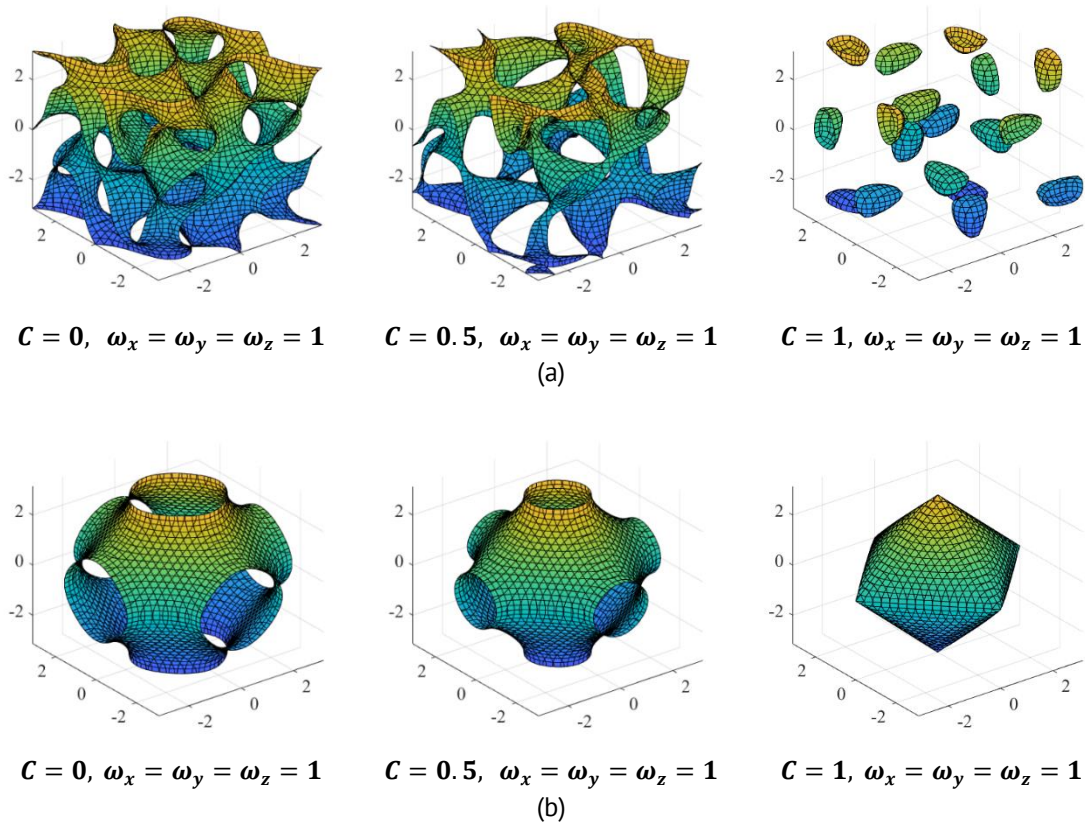


Fig. 2. Surface structures of Fischer Koch (a) and Schwarz P (b) TPMS types at different values of constant C and fixed repetition rate

The frequencies ω_x , ω_y and ω_z in the arguments of the equations of the triply periodic surface structures determine the spatial step along the corresponding coordinates. This makes it possible to fit a different number of surfaces into the periodicity cell of the metamaterial, thus changing the volume fraction or density of the material (Fig. 3). The frequency expressions have the following form:

$$\omega_x = \frac{2\pi}{L_x}, \omega_y = \frac{2\pi}{L_y}, \omega_z = \frac{2\pi}{L_z}, \quad (11)$$

where L_x, L_y, L_z are lengths of the sides of a parallelepiped defining the elementary representative cell of the metamaterial.

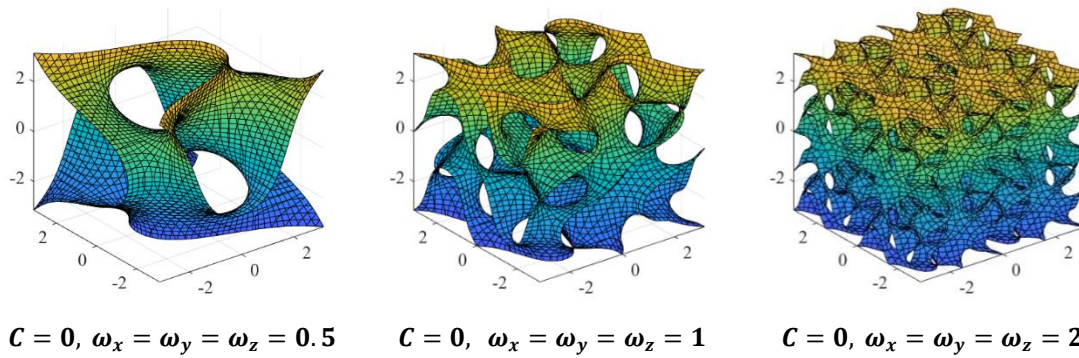


Fig. 3. Surface structures based on Fischer Koch TPMS's at different values of repetition rate and fixed constant $C = 0$

Due to the analytical expressions, the range, curvature and period of the TPMS can be easily controlled. In addition, complex calculations such as logic value, modulation and convolution can also be realised on the basis of functions describing the TPMS.

Finite element modelling of unit cells of metamaterials

The finite element model of a periodicity cell of a metamaterial based on TPMS should be constructed in such a way that the nodes of three-dimensional finite elements on the opposite faces of the cell coincide at parallel transfer of the cell along the coordinate axes by the value of the linear size of the cell. This is necessary to ensure correct formulation of periodic boundary conditions [39]. In the algorithm developed by us, the coincidence of opposite faces is ensured by duplicating three mutually perpendicular faces of the unit cell with subsequent joining of the inner surface of the surface structure. The use of this approach is caused by the unavailability of solid-state geometry of the initial TPMS-based unit cells and the absence of geometrically identical faces opposite to each other.

Let us consider more in detail the algorithm for constructing the metamaterial periodicity cell model based on a triply periodic minimal surface of the Fischer Koch type, which is required for finite element analysis. Let the volume fraction of the material, or relative density, be equal to 0.5.

Altair Sulis software [42] allows to select the desired type of surface structure, set the dimensions of the unit cell of the metamaterial based on the selected type of TPMS and the value of the volume fraction of the solid phase (Fig. 4).

The next step is to export the obtained geometry to a file of standard geometric surface description format STL (stereolithography), which can be opened by CAD software. In particular, we used the CAD package of direct geometric modelling Ansys SpaceClaim [43] for further geometry processing and preparation of the 3D solid model. In the environment of SpaceClaim, by intersecting surface structures with a $5 \times 5 \times 5$ mm cube, the required solid-state periodicity cell of the considered metamaterial was obtained (Fig. 5). In addition, three faces of the unit cell parallel to the three coordinate planes were identified, which is related to the setting periodic boundary conditions in finite element calculations.

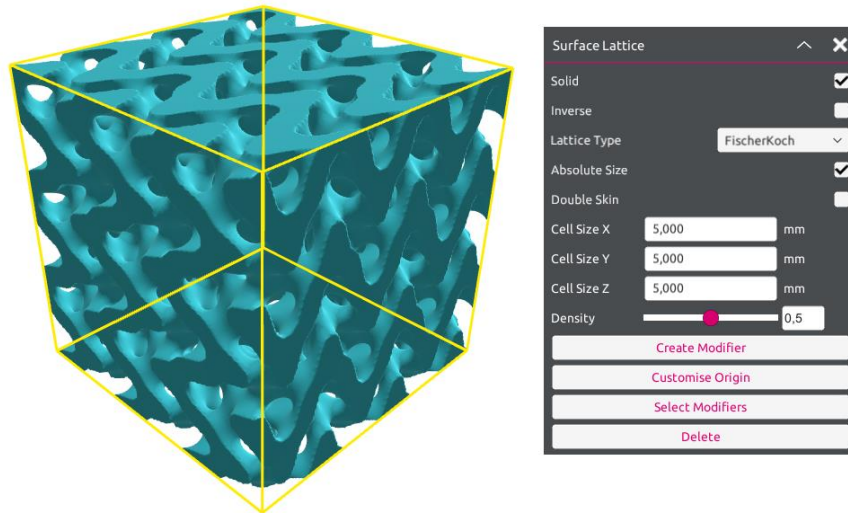


Fig. 4. The structure consisting of $3 \times 3 \times 3$ elementary cells of metamaterial with the size of $5 \times 5 \times 5$ mm, developed in Altair Sulis software on the basis of Fischer Koch surface cell with the volume fracture of solid phase equal to 0.5

The obtained model (Fig. 5) in a standard solid modelling format is exported to a finite element analysis package. In our case, the Abaqus CAE [44] was used. In Abaqus CAE, using virtual topology and setting the number of elements on the edges of the geometry, it is possible to ensure the coincidence of element nodes on the edges when duplicating the faces, which allows to guarantee the correct connection of opposite faces for subsequent work with periodic boundary conditions. The solid-air interface surface is then added to the unit cell faces in SpaceClaim (Fig. 6).

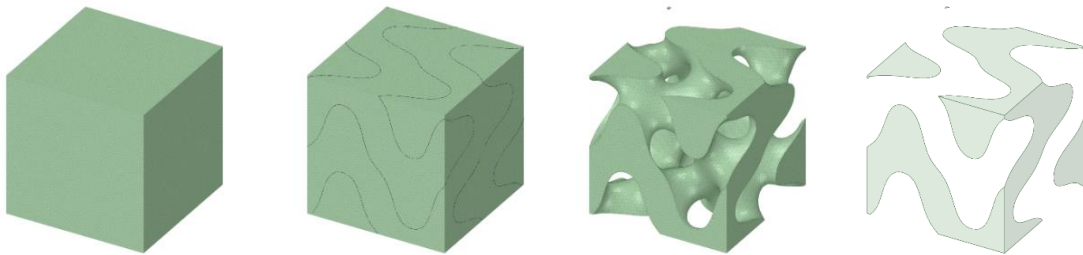


Fig. 5. Scheme of preparing the periodicity unit cell faces of metamaterial based on Fischer Koch surface structure with solid phase volume content of 0.5

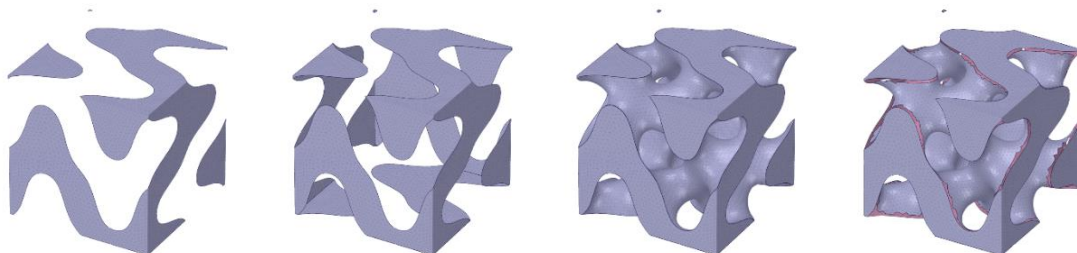


Fig. 6. Steps of construction of periodicity cell of metamaterial based on Fischer Koch surface structure with volume fraction of solid phase phase equal to 0.5

Then in Autodesk Meshmixer [45] we invert the normals of the duplicated faces and remove the elements of the inner surface close to the outer faces of the cell. Finally, in Altair SimLab software [46] we mesh the faces and the interface surface by adding elements according to the existing nodes. As a result of these operations, we obtain the volumetric mesh geometry of the unit cell of the metamaterial, the coincidence of the opposite sides of which guarantees the possibility of correct imposition of periodicity conditions between the nodes of the finite element mesh (Fig. 6).

Using the described algorithm, finite element models of metamaterial periodicity unit cells were developed for the considered surface types (Table 1). The overall dimensions of elementary cells of each type were taken as $5 \times 5 \times 5$ mm. For each type of surface structures, five options of the models were constructed with the range of volume fractions varied from 0.1 to 0.9 with a fixed step of 0.2.

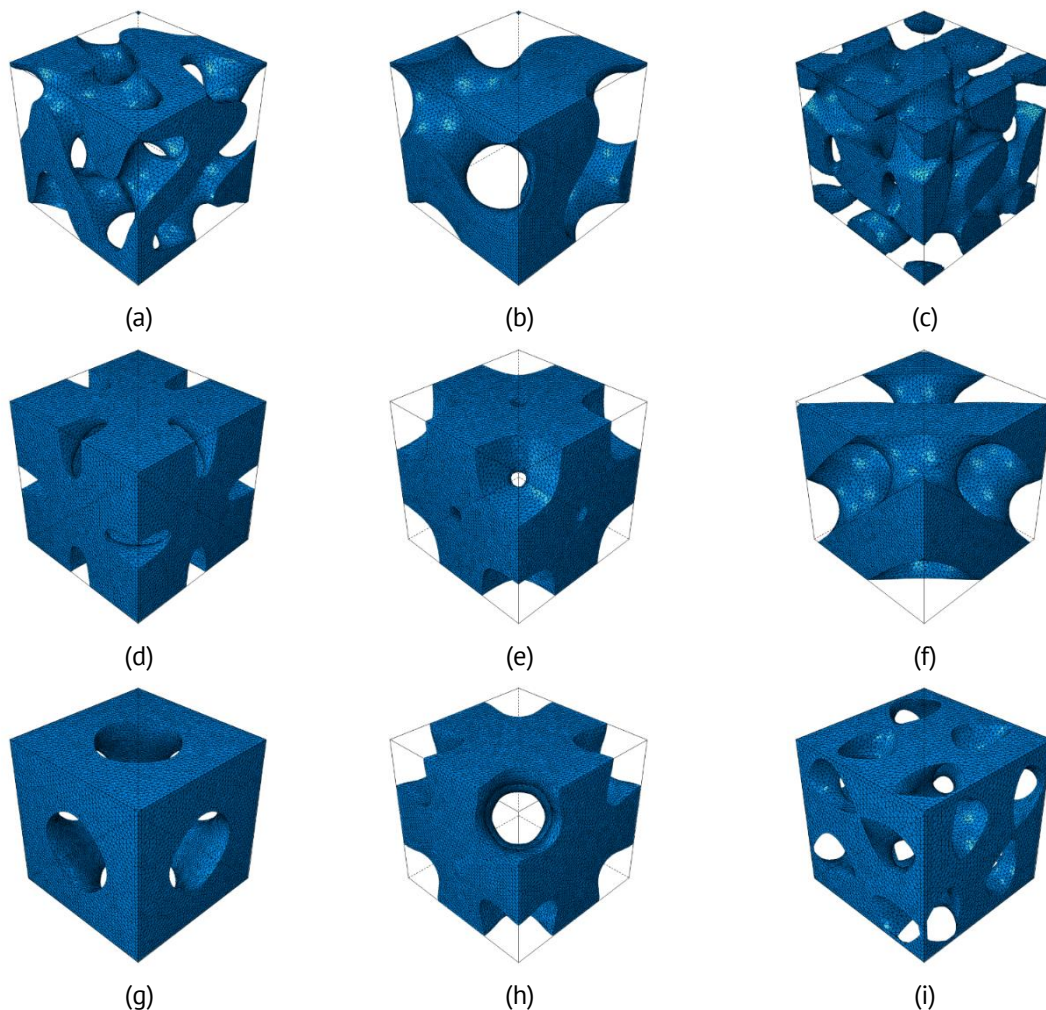


Fig. 7. Finite element models based on TPMS's with the volume fraction value of 0.5: (a) Fischer Koch; (b) Gyroid; (c) Lidinoid; (d) Neovius; (e) Primary IWP; (f) Schwarz D; (g) Schwarz P; (h) Secondary IWP; (i) Split P

Three-dimensional numerical models of periodicity cells are formed by tetrahedral linear finite elements with the first order of displacement interpolation. The characteristic side size of the finite element is 0.1 mm. The quantitative characteristics of the developed

finite element models for the case of material volume fraction equal to 0.5 are listed in Table 2, and their shape is shown in Fig. 7.

Table 2. Characteristics of the developed finite element models

Type of the unit cell	Number of elements	Number of nodes
Fischer Koch	226 999	46 101
Gyroid	237 683	46 134
Lidinoid	308 027	65 490
Neovius	236 782	48 042
Primary IWP	277 099	54 197
Schwarz D	231 803	45 569
Schwarz P	225 452	43 865
Secondary IWP	219 745	43 874

For the formulation of problems of the theory of elasticity, it is necessary to specify the material properties. In the present work, surface-type metamaterials made of isotropic aluminium are considered. The material parameters of the solid phase and air used in the calculation are presented in Table 3.

Table 3. Material properties of the solid phase and air

Material type	Young's modulus, MPa	Shear modulus, MPa	Poisson's ratio	Density, g/cm ³
Aluminium	78 670	29 700	0.32	2.67
Air	1	0.385	0.3	0.0012

Results and Discussion

This section presents the results of calculation of the elastic constants of all types of metamaterials using the direct numerical homogenisation method when varying the degree of filling of the structural unit cell with solid material.

For clarity, as an example of solving problems with periodic boundary conditions, Fig. 8 shows the results of the stress-strain state of a Fischer Koch-type unit cell at a material volume fraction value of 0.5 in tension along the Z-axis with boundary conditions (9b) and shear in the YZ-plane with boundary conditions (10c).

To analyse the effective elastic properties of the metamaterial formed by different types of elementary cells on the basis of TPMS obtained from the results of numerical homogenisation, we present comparative graphs that reflect the dependences of mechanical properties on the volume fraction of the solid phase (Fig. 9). The graphs of Young's moduli and shear moduli are given in relative units with respect to the modulus of the base material forming the solid phase of the metamaterial.

The calculations resulted in the same values of effective Young's moduli along the coordinate axes, shear moduli and Poisson's ratios in the coordinate planes. Therefore, Fig. 9 shows plots of Young's moduli along arbitrary coordinate axis, shear moduli and Poisson's ratios in arbitrary coordinate planes. The equality of Young's moduli, shear moduli and Poisson's ratios in the principal axes does not mean that the metamaterial is isotropic, since the metamaterial inherits the properties of material symmetry, which should lead to the syngonic material behaviour with cubic symmetry. Below this issue will be considered in more detail.

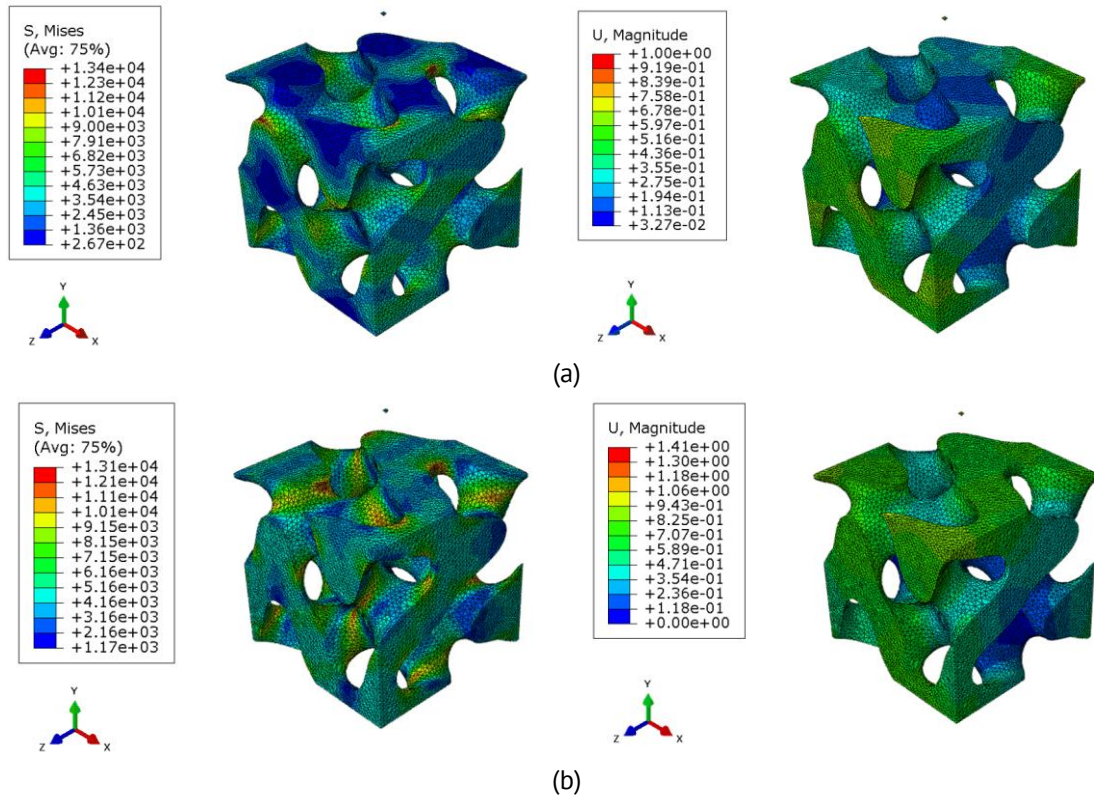


Fig. 8. Equivalent stresses (left) and total displacement (right) under uniaxial tension along the Z-axis (a) and shear in the YZ-plane (b) at the meso-level of a metamaterial based on a Fischer Koch surface structure with a volume fraction of 0.5

The dependences of Young's moduli (Fig. 9(a)) and shear moduli values (Fig. 9(b)) are qualitatively similar for each type of elementary cells of the metamaterial. At the material volume fraction of 0.0, the diagrams reflect the values of mechanical characteristics of air, while at the volume fraction of 1.0 they coincide with the values of elastic moduli of aluminium. As the volume fraction of the solid phase of the metamaterial increases, the values of Young's and shear moduli grow and tend to the values of elastic properties of the base material.

The intensity of change in mechanical properties at the same rate of change in volume fraction is different for each cell type. It is interesting to mention that the Neovius and Lidinoid cell types show a minimum growth of Young's modulus in the first third of the volume fraction range, which is explained by the lack of cohesion of the cell geometry at the described values of the effective density of the metamaterial.

Note that all the considered types of metamaterials show strongly nonlinear dependence of elastic properties on relative density, which differs from simple formulas, for example, in the mechanics of mixtures. Moreover, the curvature is more pronounced for values of relative density less than 0.5. This may indicate a more significant influence of the topological characteristics of the cell on its behaviour compared to their influence in the case of high relative density, where the mechanical properties of the basic material are the prevailing factor. It can be concluded that for problems with relative density close to 1.0 the question of choosing a particular type of cell is not so relevant, and that in a comparative study of different topological characteristics the results obtained for small values of relative density will be more indicative.

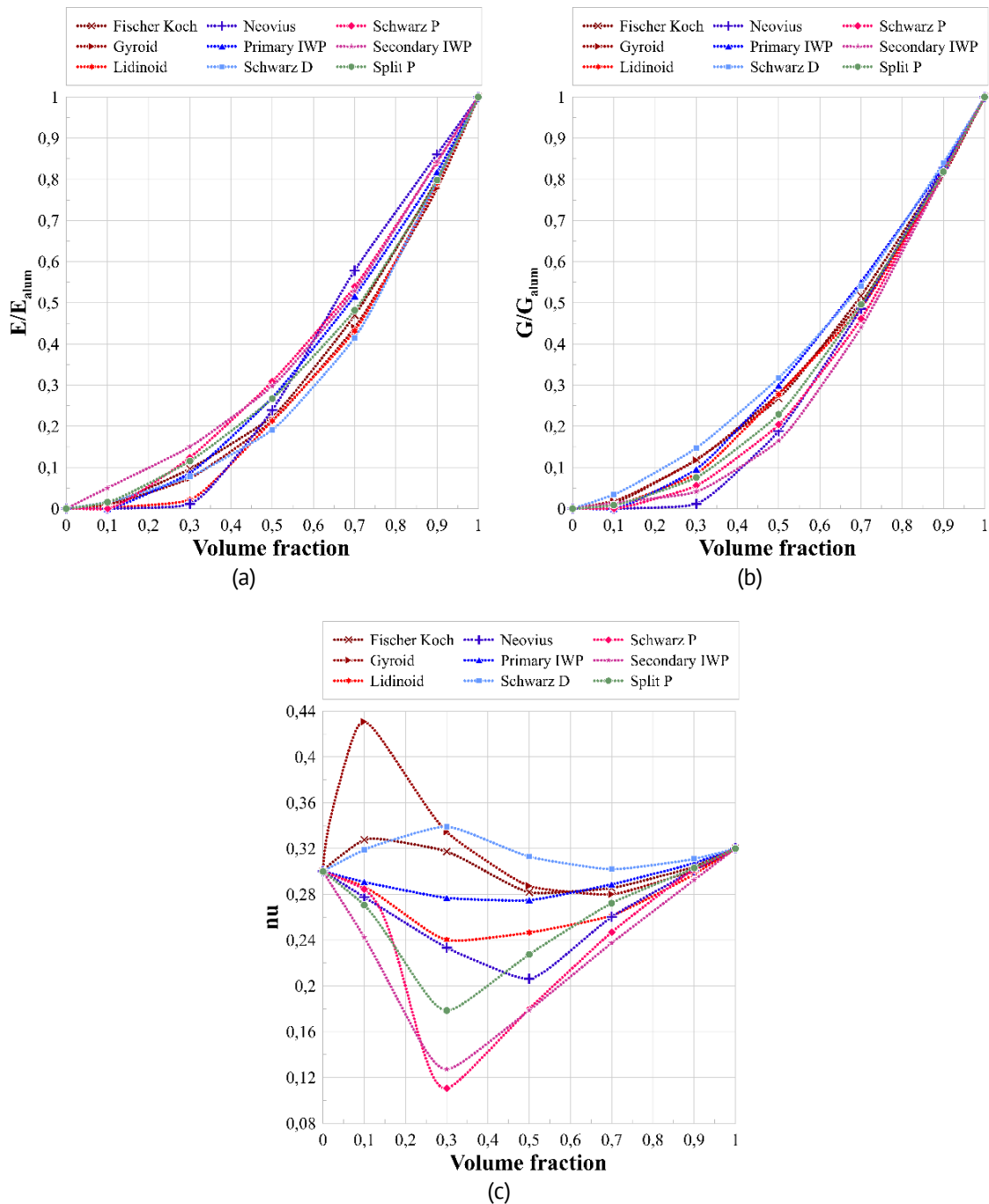


Fig. 9. Dependences of effective elastic constants of metamaterial based on nine types of surface structures on the volume content of solid phase: (a) Young's moduli; (b) shear moduli; (c) Poisson's ratios

When analysing the dependences of Poisson's ratio values (Fig. 9(c)), much less consistency in the qualitative behaviour of the plots for different types of metamaterials is observed. For values of the volume fraction greater than 0.5, a general tendency for the final value to tend to the value of the constant for the solid material is revealed. The reasons for such an effect were discussed earlier. At the same time, the values of the constant in the range of volume fraction 0.1-0.5 are non-monotonic. The reason for this phenomenon may be a more pronounced influence of the topology of the unit cell on the transverse deformations. The consequence of this phenomenon is the apparent presence of stationary points corresponding to the maximum or minimum achievable values of the

Poisson's ratio, which can be useful in problems where its value has a significant influence on the global result. It can also be noticed that Gyroid, Fischer Koch, Schwarz P unit cells at medium values of effective density show a larger value of Poisson's ratio in comparison with the value of Poisson's ratio of air and other types of unit cells with a much smaller value of this dimensionless characteristic.

The graphs shown in Fig. 9 may give a wrong idea about the isotropy of the effective properties of the obtained metamaterials. To assess the degree of anisotropy and to check the relationship of mechanical properties between each other, we determine from the available values of Young's modulus and shear modulus the value of Poisson's ratio for each unit cell in accordance with the classical formula for an isotropic continuous medium: $\nu = \frac{E}{2G} - 1$. The results of the calculations are presented in Fig. 10.

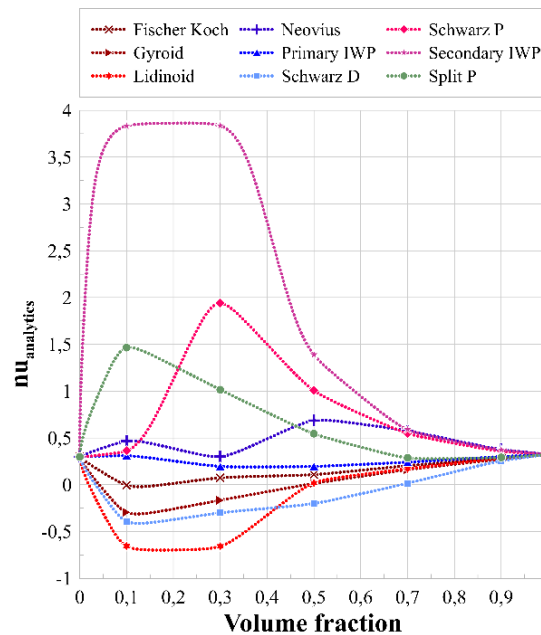


Fig. 10. Dependences of the effective Poisson's ratios calculated by the isotropic continuum model formula on the volume fraction of the solid phase of the metamaterial

The graphs (Fig. 10) clearly show that the obtained analytical values according to the classical formula of the isotropic material model both qualitatively and quantitatively differ from the calculated parameters. This means that the hypothesis of the syngonic material behaviour with cubic symmetry implemented into orthotropic model of the metamaterial is confirmed, because despite the equality of Young's moduli and shear moduli in the directions of the three principal axes, the basic relation about the relation between these constants for an isotropic material is not fulfilled. At the same time, the coincidence of the values of elastic moduli along the three principal axes can be explained by the order of spatial symmetry of the unit cell of the metamaterial on the basis of the considered types of surface structures.

Conclusion

The presented work considers models of metamaterials based on triply periodic minimal surfaces, which is a popular and rational direction in digital materials science. A computerized technique for constructing periodicity cells of metamaterials as representative volume elements of specific heterogeneous media is proposed.

The boundary value problems for uniaxial tension and pure shear for calculating the stress-strain state of the selected representative volume elements taking into account periodic boundary conditions are formulated and finite element models are developed.

Using a direct numerical homogenization method at the meso-level of the periodicity cell, the elastic properties of metamaterials are calculated. A number of assumptions about the relationship between mechanical properties and the topology parameters of the basic cells of TPMS-metamaterials, such as the type of unit cell and the volume fraction of the material, have been verified. Dependences of effective properties on volume fraction of solid material are revealed and it is noted that for their correct description, due to syngonic material behaviour with cubic symmetry, application of orthotropic material model is required. It is shown that the considered types of surface metamaterials exhibit strongly nonlinear dependence of elastic properties on the relative density or volume fraction of the solid phase of the metamaterial. The analysis of Poisson's ratios shows a significant difference in their behaviour for different types of metamaterials, which may be caused by a more pronounced influence of the unit cell topology on the transverse deformations.

The conducted study of dependences should allow to create TPMS-materials with specific mechanical properties necessary for the development of modern promising and advanced industrial products, including medical applications.

References

1. Popovich AA, Sufiiarov VS, Borisov EV, Polozov IA, Masaylo DV. Design and manufacturing of tailored microstructure with selective laser melting. *Materials Physics and Mechanics*. 2018;38(1): 1–10.
2. Torquato S, Gibiansky L, Silva M, Gibson L. Effective mechanical and transport properties of cellular solids. *Int. J. Mech. Sci.* 2000;40(1): 71–82.
3. Christensen RM. Mechanics of cellular and other low-density materials. *Int. J. Sol. Struct.* 2000;37(1–2): 93–104.
4. de Jonge CP, Kolken HMA, Zadpoor AA. Non-Auxetic Mechanical Metamaterials. *Materials*. 2019;12(4): 635.
5. Kolken HMA, Zadpoor AA. Auxetic Mechanical Metamaterials. *RSC Advances*. 2017;7: 5111–5129.
6. Comi C, Moscatelli M, Marigo JJ. Two scale homogenization in ternary locally resonant metamaterials. *Materials Physics and Mechanics*. 2020;44(1): 8–18.
7. Walser RM. Electromagnetic Metamaterials. *Proceedings of SPIE. Complex Mediums II: Beyond Linear Isotropic Dielectrics*. 2001;4467: 1–15.
8. Maslov LB. Study of vibrational characteristics of poroelastic mechanical systems. *Mechanics of Solids*. 2012;47(2): 221–233.
9. Zadpoor AA. Design for additive bio-manufacturing: from patient-specific medical devices to rationally designed meta-biomaterials. *Int. J. Mol. Sci.* 2017;18(8): 1607.
10. Maslov LB. Mathematical model of bone regeneration in a porous implant. *Mechanics of Composite Materials*. 2017;53(3): 399–414.
11. Fousová M, Vojteěch D, Kubásek J, Jablonská E, Fojt J. Promising characteristics of gradient porosity Ti-6Al-4V alloy prepared by SLM process. *J. Mech. Behav. Biomed. Mater.* 2017;69: 368–376.
12. Bobbert FSL, Janbaz S, Zadpoor AA. Towards deployable meta-implants. *Journal of Materials Chemistry. B*. 2018;6(21): 3449–3455.

13. Kolken HM, Janbaz S, Leeflang SM, Lietaert K, Weinans HH, Zadpoor AA. Rationally designed meta-implants: a combination of auxetic and conventional meta-biomaterials. *Mater. Horiz.* 2018;5(1): 28–35.
14. Hanks B, Berthel J, Frecker M, Simpson TW. Mechanical properties of additively manufactured metal lattice structures: data review and design interface. *Addit. Manuf.* 2020;35: 101301.
15. Feng J, Fu J, Shang C, Lin Z, Li B. Porous scaffold design by solid T-splines and triply periodic minimal surfaces. *Comput. Methods Appl. Mech. Eng.* 2018;336: 333–352.
16. Zadpoor AA, Hedayati R. Analytical relationships for prediction of the mechanical properties of additively manufactured porous biomaterials. *J. Biomed. Mater. Res. Part A.* 2016;104(12): 3164–3174.
17. Hedayati R, Sadighi M, Mohammadi-Aghdam M, Zadpoor A. Mechanical properties of regular porous biomaterials made from truncated cube repeating unit cells: analytical solutions and computational models. *Mat. Sci. Eng.* 2016;60: 163–183.
18. Vlădulescu F, Constantinescu DM. Lattice structure optimization and homogenization through finite element analyses. *Proceedings of the Institution of Mechanical Engineers, Part L: Journal of Materials: Design and Applications.* 2020;234: 1490–1502.
19. Ravari MK, Kadkhodaei M, Badrossamay M, Rezaei R. Numerical investigation on mechanical properties of cellular lattice structures fabricated by fused deposition modelling. *Int. J. Mech. Sci.* 2014;88: 154–161.
20. Zhmaylo M, Maslov L, Borovkov A, Tarasenko F. Finite element homogenization and experimental evaluation of additively manufactured lattice metamaterials. *J. Braz. Soc. Mech. Sci. Eng.* 2023;45: 299.
21. Feng JW, Fu JZ, Yao XH, He Y. Triply periodic minimal surface (TPMS) porous structures: from multi-scale design, precise additive manufacturing to multidisciplinary applications. *Int. J. Extrem. Manuf.* 2022;4: 022001.
22. Mitrofanov AV, Maslov LB, Mizonov VE. A stochastic model of cell transformations at bone tissue regeneration. *Rus. J. Biomech.* 2021;25(1): 41–54.
23. Maslov LB, Dmitryuk AY, Zhmaylo MA, Tarasenko FD, Kovalenko AN. Strength analysis in a hip endoprosthesis made of polymeric material. *Rus. J. Biomech.* 2022;26(4): 14–28.
24. Chikova TN, Kichenko AA, Tverier VM, Nyashin YI. Biomechanical modelling of trabecular bone tissue in remodelling equilibrium. *Rus. J. Biomech.* 2018;22(3): 245–253.
25. Kichenko AA. Cancellous bone tissue remodelling: mathematical modelling. *Rus. J. Biomech.* 2019;23(3): 284–304.
26. Maslov LB. Biomechanical model and numerical analysis of tissue regeneration within a porous scaffold. *Mechanics of Solids.* 2020;55(7): 1115–1134.
27. Callens SJP, Arns CH, Kuliesh A, Zadpoor AA. Decoupling minimal surface metamaterial properties through multi-material hyperbolic tilings. *Adv. Funct. Mater.* 2021;31: 2101373.
28. Maslov LB. Dynamic Model of a Periodic Medium with Double Porosity. *Mechanics of Solids.* 2018;53(2): 184–194.
29. Deng B, Cheng GJ. Soap film inspired mechanical metamaterials approaching theoretical bound of stiffness across full density range. *Mater. Horiz.* 2021;8: 987–996.
30. Maskery I, Sturm L, Aremu AO, Panesar A, Williams CB, Tuck CJ, Wildman RD, Ashcroft IA, Hague RJM. Insights into the mechanical properties of several triply periodic minimal surface lattice structures made by polymer additive manufacturing. *Polymer.* 2018;152: 62–71.
31. Lee DW, Khan KA, Abu Al-Rub RK. Stiffness and yield strength of architected foams based on the Schwarz primitive triply periodic minimal surface. *Int. J. Plast.* 2017;95: 1–20.
32. Al-Ketan O, Soliman A, Al-Qubaisi AM, Abu Al-Rub RK. Nature-inspired lightweight cellular co-continuous composites with architected periodic gyroidal structures. *Adv. Eng. Mater.* 2018;20: 1700549.
33. Feng J, Liu B, Lin Z, Fu J. Isotropic porous structure design methods based on triply periodic minimal surfaces. *Mater. Des.* 2021;210: 110050.
34. Akifyev KN, Kharin NV, Statsenko EO, Sachenkov OA, Bolshakov PV. Pilot study of lattice endoprosthesis buckling by compression in-situ using X-ray tomography. *Rus. J. Biomech.* 2023;27(4): 32–39.
35. Bolshakov P, Raginov I, Egorov V, Kashapova R, Kashapov R, Baltina T, Sachenkov O. Design and optimization lattice endoprosthesis for long bones: manufacturing and clinical experiment. *Materials.* 2020;13(5): 1185.
36. Kharin N, Bolshakov P, Kuchumov AG. Numerical and Experimental Study of a Lattice Structure for Orthopedic Applications. *Materials.* 2023;16(2): 744.
37. Bolshakov P, Kuchumov AG, Kharin N, Akifyev K, Statsenko E, Silberschmidt V. Method of computational design for additive manufacturing of hip endoprosthesis based on basic-cell concept. *Int. J. Numer. Meth. Biomed. Engng.* 2024;40(3): 3802.

38. Montazerian H, Davoodi E, Asadi-Eydivand M, Kadkhodapour J, Solati-Hashjin M. Porous scaffold internal architecture design based on minimal surfaces: a compromise between permeability and elastic properties. *Mater. Des.* 2017;126: 98–114.
39. Omairey SL, Dunning PD, Sriramula S. Development of an ABAQUS plugin tool for periodic RVE homogenisation. *Engineering with Computers.* 2019;35: 567–577.
40. Karakoç A. RegionTPMS – Region based triply periodic minimal surfaces (TPMS) for 3-D printed multiphase bone scaffolds with exact porosity values. *SoftwareX.* 2021;16: 100835.
41. Al-Ketan O, Abu Al-Rub RK. MSLattice: A free software for generating uniform and graded lattices based on triply periodic minimal surfaces. *Mat. Design. Process. Comm.* 2020: 205.
42. *Design software for additive manufacturing.* Available from: <https://gen3d.com> [Accessed 1 June 2023].
43. *Ansys SpaceClaim. 3D Modeling Software.* Available from: <https://www.ansys.com/products/3d-design/ansys-spaceclaim> [Accessed 1 June 2023].
44. *Abaqus CAE. A powerful standalone interface.* Available from: <https://www.simuleon.com/simulia-abaqus/abaqus-cae> [Accessed 1 June 2023].
45. *Autodesk Meshmixer. Free software for making awesome stuff.* Available from: <https://www.meshmixer.com> [Accessed 1 June 2023].
46. *Multiphysics Workflows with CAD Associativity | Altair SimLab.* Available from: <https://altair.com/simlab> [Accessed 1 June 2023].

About Author

Aleksey I. Borovkov  

Candidate of Technical Sciences, Professor

Vice-rector for Digital Transformation (Peter the Great St. Petersburg Polytechnic University, St. Petersburg, Russia)

Leonid B. Maslov  

Doctor of Physical and Mathematical Sciences, Professor

Lead Researcher (Peter the Great St. Petersburg Polytechnic University, St. Petersburg, Russia)

Lead Researcher (Ivanovo State Power Engineering University n.a. V.I. Lenin, Ivanovo, Russia)

Mikhail A. Zhmaylo  

Master of Science

Lead Engineer (Peter the Great St. Petersburg Polytechnic University, St. Petersburg, Russia)

Fedor D. Tarasenko  

Master of Science

Lead Engineer (Peter the Great St. Petersburg Polytechnic University, St. Petersburg, Russia)

Liliya S. Nezhinskaya  

Bachelor of Science

Engineer (Peter the Great St. Petersburg Polytechnic University, St. Petersburg, Russia)